baculovirus-expressed recombinant desmogleins. J Immunol. 1997; 159:2010–2017. [PubMed: 9257868]

Pathophysiology of blister formation in pemphigus

Pemphigus antibodies cause steric hindrance

63. Koch PJ, Mahoney MG, Ishikawa H, Pulkkinen L, Uitto J, Shultz L, et al. Targeted disruption of the pemphigus vulgaris antigen (desmoglein 3) gene in mice causes loss of keratinocyte cell adhesion with a phenotype similar to pemphigus vulgaris. J Cell Biol. 1997; 137:1091–1102. [PubMed: 9166409]

64. Mahoney MG, Wang Z, Rothenberger K, Koch PJ, Amagai M, Stanley JR. Explanations for the clinical and microscopic localization of lesions in pemphigus foliaceus and vulgaris. J Clin Invest. 1999; 103:461–468. [PubMed: 10021453]

65. Sekiguchi M, Futei Y, Fujii Y, Iwasaki T, Nishikawa T, Amagai M. Dominant autoimmune epitopes recognized by pemphigus antibodies map to the N-terminal adhesive region of desmogleins. J Immunol. 2001; 167:5439–5448. [PubMed: 11673563]

66. Li N, Aoki V, Hans-Filho G, Rivitti EA, Diaz LA. The role of intramolecular epitope spreading in the pathogenesis of endemic pemphigus foliaceus (fogo selvagem). J Exp Med. 2003; 197:1501–1510. [PubMed: 12771179]

Pemphigus antibodies cause intracellular signaling

67. Caldelari R, de Bruin A, Baumann D, Suter MM, Bierkamp C, Balmer V, Müller E. A central role for the armadillo protein plakoglobin in the autoimmune disease pemphigus vulgaris. J Cell Biol. 2001; 153:823–834. [PubMed: 11352942]

68. Berkowitz P, Hu P, Liu Z, Diaz LA, Enghild JJ, Chua MP, Rubenstein DS. Desmosome signaling. Inhibition of p38MAPK prevents pemphigus vulgaris IgG-induced cytoskeleton reorganization. J Biol Chem. 2005; 280:23778–23784. [PubMed: 15840580]

69. Rubenstein DS, Diaz LA. Pemphigus antibody induced phosphorylation of keratinocyte proteins. Autoimmunity. 2006; 39:577–586. [PubMed: 17101501]

70. Chernyavsky AI, Arredondo J, Kitajima Y, Sato-Nagai M, Grando SA. Desmoglein versus non-desmoglein signaling in pemphigus acantholysis: characterization of novel signaling pathways downstream of pemphigus vulgaris antigens. J Biol Chem. 2007; 282:13804–13812. [PubMed: 17344213]

71. Berkowitz P, Chua M, Liu Z, Diaz LA, Rubenstein DS. Autoantibodies in the autoimmune disease pemphigus foliaceus induce blistering via p38 mitogen-activated protein kinase-dependent signaling in the skin. Am J Pathol. 2008; 173:1628–1636. [PubMed: 18988808]

72. Jolly PS, Berkowitz P, Bektas M, Lee HE, Chua M, Diaz LA, Rubenstein DS. p38MAPK signaling and desmoglein-3 internalization are linked events in pemphigus acantholysis. J Biol Chem. 2010; 285:8936–8941. [PubMed: 20093368]

73. Mao X, Sano Y, Park JM, Payne AS. p38 MAPK activation is downstream of the loss of intercellular adhesion in pemphigus vulgaris. J Biol Chem. 2011; 286:1283–1291. [PubMed: 21078676]

74. Williamson L, Raess NA, Caldelari R, Zakher A, de BA, Posthaus H, Bolli R, Hunziker T, Suter MM, Muller EJ. Pemphigus vulgaris identifies plakoglobin as key suppressor of c-Myc in the skin. EMBO J. 2006; 25:3298–3309. [PubMed: 16871158]

75. Delva E, Jennings JM, Calkins CC, Kottke MD, Faundez V, Kowalczyk AP. Pemphigus vulgaris IgG-induced desmoglein-3 endocytosis and desmosomal disassembly are mediated by a clathrin- and dynamin-independent mechanism. J Biol Chem. 2008; 283:18303–18313. [PubMed: 18434319]

Immunology of development of anti-desmoglein antibodies

76. Wucherpfennig KW, Yu B, Bhol K, Monos DS, Argyris E, Karr RW, Ahmed AR, Strominger JL. Structural basis for major histocompatibility complex (MHC)-linked susceptibility to

autoimmunity: charged residues of a single MHC binding pocket confer selective presentation of self-peptides in pemphigus vulgaris. Proc Natl Acad Sci U S A. 1995; 92:11935–11939. (First identification of desmoglein 3-specific T cells in human). [PubMed: 8524878]

77. Lin MS, Swartz SJ, Lopez A, Ding X, Fernandez-Vina MA, Stastny P, Fairley JA, Diaz LA. Development and characterization of desmoglein-3 specific T cells from patients with pemphigus vulgaris. J Clin Invest. 1997; 99:31–40. [PubMed: 9011573]
78. Amagai M, Tsunoda K, Suzuki H, Nishifuji K, Koyasu S, Nishikawa T. Use of autoantigen-knockout mice in developing an active autoimmune disease model for pemphigus. J Clin Invest. 2000; 105:625–631. (Development of active disease mouse model for pemphigus vulgaris). [PubMed: 10712434]
79. Tsunoda K, Ota T, Aoki M, Yamada T, Nagai T, Nakagawa T, Koyasu S, Nishikawa T, Amagai M. Induction of pemphigus phenotype by a mouse monoclonal antibody against the amino-terminal adhesive interface of desmoglein 3. J Immunol. 2003; 170:2170–2178. (Pathogenic monoclonal antibodies against desmoglein 3 was isolated). [PubMed: 12574390]
80. Takahashi H, Amagai M, Nishikawa T, Fujii Y, Kawakami Y, Kuwana M. Novel system evaluating in vivo pathogenicity of desmoglein 3-reactive T cell clones using murine pemphigus vulgaris. J Immunol. 2008; 181:1526–1535. [PubMed: 18606708]

Desmogleins are targets in infectious diseases

81. Melish ME, Glasgow LA. The staphylococcal scalded-skin syndrome. Development of an experimental model. N Engl J Med. 1970; 282:1114–1119. (Exfoliative toxin causes a blister in neonatal mice). [PubMed: 4245327]
82. Dancer SJ, Garratt R, Saldanha J, Jhoti H, Evans R. The epidermolytic toxins are serine proteases. FEBS Letters. 1990; 268:129–132. [PubMed: 2384148]
83. Vath GM, Earhart CA, Rago JV, Kim MH, Bohach GA, Schlievert PM, Ohlendorf DH. The structure of the superantigen exfoliative toxin A suggests a novel regulation as a serine protease. Biochemistry. 1997; 36:1559–1566. (Exfoliative toxin may cleave a specific protein receptor.). [PubMed: 9048539]
84. Cavarelli J, Prevost G, Bourguet W, Moulinier L, Chevrier B, Delagoutte B, Bilwes A, Mourey L, Rifai S, Piemont Y, et al. The structure of Staphylococcus aureus epidermolytic toxin A, an atypic serine protease, at 1.7A resolution. Structure. 1997; 5:813–824. [PubMed: 9261066]
85. Amagai M, Matsuyoshi N, Wang ZH, Andl C, Stanley JR. Toxin in bullous impetigo and staphylococcal scalded-skin syndrome targets desmoglein 1. Nature Med. 2000; 6:1275–1277. [PubMed: 11062541]
86. Hanakawa Y, Schechter NM, Lin C, Nishifuji K, Amagai M, Stanley JR. Enzymatic and molecular characteristics of the efficiency and specificity of exfoliative toxin cleavage of desmoglein 1. J Biol Chem. 2004; 279:5268–5277. [PubMed: 14630910]
87. Wang H, Li ZY, Liu Y, Persson J, Beyer I, Moller T, Koyuncu D, Drescher MR, Strauss R, Zhang XB, Wahl JK 3rd, Urban N, Drescher C, Hemminki A, Fender P, Lieber A. Desmoglein 2 is a receptor for adenovirus serotypes 3, 7, 11 and 14. Nat Med. 2011; 17:96–104. [PubMed: 21151137]

Desmogleins are targets in genetic diseases

88. Kljuic A, Bazzi H, Sundberg JP, Martinez-Mir A, O'Shaughnessy R, Mahoney MG, Levy M, Montagutelli X, Ahmad W, Aita VM, et al. Desmoglein 4 in hair follicle differentiation and epidermal adhesion: evidence from inherited hypotrichosis and acquired pemphigus vulgaris. Cell. 2003; 113:249–260. (Desmoglein 4 associated with localized autosomal recessive hypothrichosis). [PubMed: 12705872]
89. Pilichou K, Nava A, Basso C, Beffagna G, Bauce B, Lorenzon A, Frigo G, Vettori A, Valente M, Towbin J, Thiene G, Danieli GA, Rampazzo A. Mutations in desmoglein-2 gene are associated with arrhythmogenic right ventricular cardiomyopathy. Circulation. 2006; 113:1171–1179. [PubMed: 16505173]

Desmogleins do more than provide adhesion of cells

90. Eshkind L, Tian Q, Schmidt A, Franke WW, Windoffer R, Leube RE. Loss of desmoglein 2 suggests essential functions for early embryonic development and proliferation of embryonal stem cells. Eur J Cell Biol. 2002; 81:592–598. [PubMed: 12494996]
91. Brennan D, Hu Y, Joubeh S, Choi YW, Whitaker-Menezes D, O'Brien T, Uitto J, Rodeck U, Mahoney MG. Suprabasal Dsg2 expression in transgenic mouse skin confers a hyperproliferative and apoptosis-resistant phenotype to keratinocytes. J Cell Sci. 2007; 120:758–771. [PubMed: 17284515]
92. Getsios S, Simpson CL, Kojima S, Harmon R, Sheu LJ, Dusek RL, Cornwell M, Green KJ. Desmoglein 1-dependent suppression of EGFR signaling promotes epidermal differentiation and morphogenesis. J Cell Biol. 2009; 185:1243–1258. [PubMed: 19546243]
93. Garrod D, Chidgey M. Desmosome structure, composition and function. Biochim Biophys Acta. 2008; 1778:572–587. [PubMed: 17854763]

The future: therapy of pemphigus based on the understanding of its pathophysiology and immunology

Anti-idiotypic therapy

94. Payne AS, Ishii K, Kacir S, Lin C, Li H, Hanakawa Y, Tsunoda K, Amagai M, Stanley JR, Siegel DL. Genetic and functional characterization of human pemphigus vulgaris monoclonal autoantibodies isolated by phage display. J Clin Invest. 2005; 115:888–899. [PubMed: 15841178]
95. Yamagami J, Kacir S, Ishii K, Payne AS, Siegel DL, Stanley JR. Antibodies to the desmoglein 1 precursor proprotein but not to the mature cell surface protein cloned from individuals without pemphigus. J Immunol. 2009; 183:5615–5621. [PubMed: 19843946]
96. Yamagami J, Payne AS, Kacir S, Ishii K, Siegel DL, Stanley JR. Homologous regions of autoantibody heavy chain complementarity-determining region 3 (H-CDR3) in patients with pemphigus cause pathogenicity. J Clin Invest. 2010; 120:4111–4117. [PubMed: 20978359]

Rituximab

97. Joly P, Mouquet H, Roujeau JC, D'Incan M, Gilbert D, Jacquot S, Gougeon ML, Bedane C, Muller R, Dreno B, et al. A single cycle of rituximab for the treatment of severe pemphigus. N Engl J Med. 2007; 357:545–552. [PubMed: 17687130]

Signaling

98. Berkowitz P, Hu P, Warren S, Liu Z, Diaz LA, Rubenstein DS. p38MAPK inhibition prevents disease in pemphigus vulgaris mice. Proc Natl Acad Sci U S A. 2006; 103:12855–12860. [PubMed: 16908851]
99. Nguyen VT, Arredondo J, Chernyavsky AI, Kitajima Y, Pittelkow M, Grando SA. Pemphigus vulgaris IgG and methylprednisolone exhibit reciprocal effects on keratinocytes. J Biol Chem. 2004; 279:2135–2146. (Corticosteroids may by therapeutic in pemphigus by increasing synthesis of desmogleins). [PubMed: 14600150]

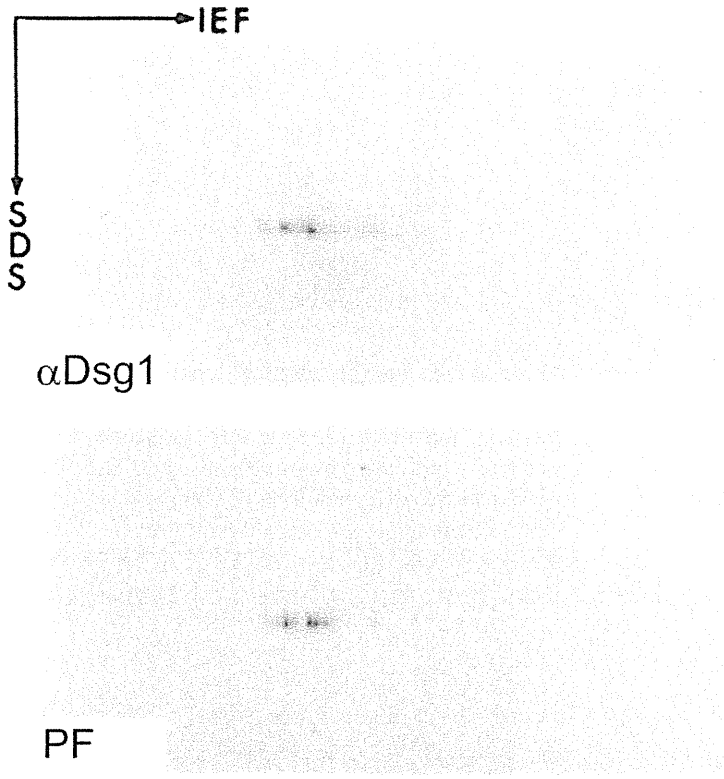

Figure 1.
One of the major pieces of evidence that desmoglein 1 is the pemphigus foliaceus antigen. 2-dimensional gel electrophoresis of extracts of epidermis followed by immunoblotting with pemphigus foliaceus serum and an anti-desmoglein 1 antibody shows that both identify spots with the same migration, convincing proof that both bind the same protein. (From, Koulu, L., Kusumi, A., Steinberg, M.S., Klaus Kovtun, V., and Stanley, J.R. 1984. Human autoantibodies against a desmosomal core protein in pemphigus foliaceus. *J. Exp. Med.* 160:1509–1518).

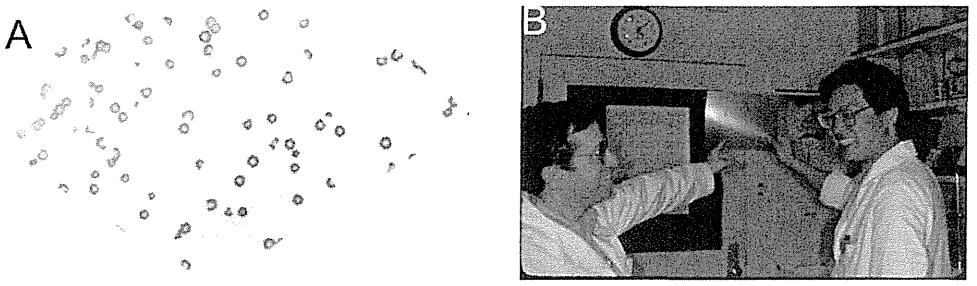

Figure 2.
Original data from the cloning of pemphigus vulgaris antigen. A) Purified λgt11 expression phage that contain cDNA for pemphigus vulgaris antigen. A single clone multiplies in bacteria, and all its offspring were blotted to nitrocellulose. All resultant clones stain positively with pemphigus vulgaris sera. The cDNA was sequenced to show that the protein produced was desmoglein 3. B) John Stanley (left) and Masayuki Amagai on the day in 1991 when the pemphigus vulgaris antigen clone was identified. (Amagai, M., Klaus-Kovtun, V., and Stanley, J.R. 1991. Autoantibodies against a novel epithelial cadherin in pemphigus vulgaris, a disease of cell adhesion. *Cell* 67:869–877.)

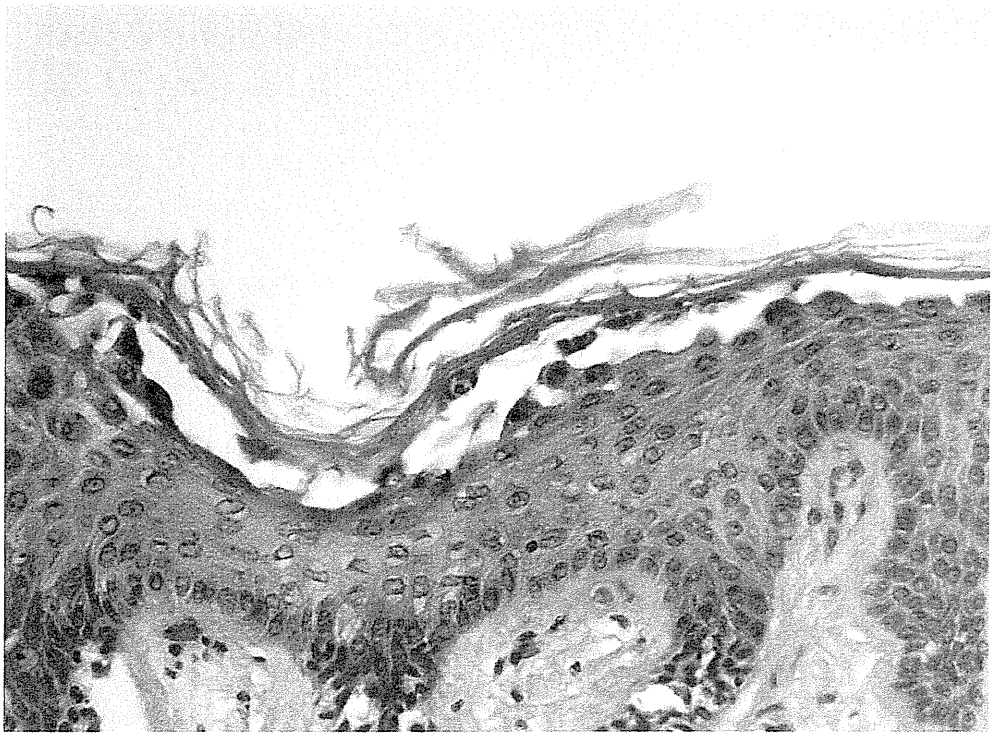

Figure 3.
A monoclonal, monovalent anti-desmoglein 1 antibody cloned from a pemphigus foliaceus patient causes typical histology of pemphigus foliaceus when injected into normal human skin organ culture.

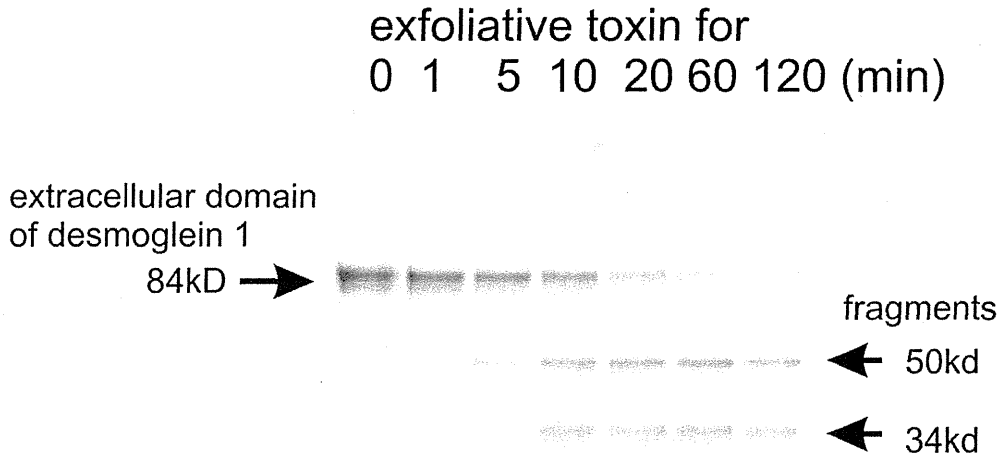

Figure 4.
Coomassie blue gel showing cleavage of the 84-kD extracellular domain of desmoglein 1 to a 50 kD and 34 kD fragment, increasing with time of incubation with exfoliative toxin A. (Hanakawa, Y., Schechter, N.M., Lin, C., Nishifuji, K., Amagai, M., and Stanley, J.R. 2004. Enzymatic and molecular characteristics of the efficiency and specificity of exfoliative toxin cleavage of desmoglein 1. *J. Biol. Chem.* 279:5268–5277.)

Table 1

Desmogleins targeted in human diseases

Isoform	Type	Diseases
desmoglein 1	autoimmune	pemphgius foliaceus pemphigus vulgaris (mucocutaneous type) paraneoplastic pemphigus
	infection	staphylococcal scalded skin syndrome bullous impetigo
	genetic	striate palmoplantar keratoderma
desmoglein 2	infection	respiratory and urinary tract infection (receptors for adenovirus serotypes 3, 7, 11, and 14)
	genetic	arrythmogenic right ventricular cardiomyopathy dilated cardiomyopathy
desmoglein 3	autoimmune	pemphigus vulgaris (mucosal dominant type, mucocutaneous type) paraneoplastic pemphigus
desmoglein 4	genetic	hypotrichosis

[10] Aberg KM, Radek KA, Choi EH, Kim DK, Demerjian M, Hupe M, et al. Psychological stress downregulates epidermal antimicrobial peptide expression and increases severity of cutaneous infections in mice. J Clin Invest 2007; 117:3339–49.

Haruka Goto[a,1,*], Maya Hongo[a,1], Hiroshi Ohshima[a], Masumi Kurasawa[a], Satoshi Hirakawa[a], Yasuo Kitajima[b]

[a]*Skin Research Department, POLA Chemical Industries, Inc., Yokohama, Japan*; [b]*Kizawa Memorial Hospital, Gifu, Japan*

*Corresponding author at: Skin Research Department, POLA Chemical Industries, Inc., 560 Kashio-cho, Totsuka-ku, Yokohama 244-0812, Japan.
Tel.: +81 45 826 7134; fax: +81 45 826 7249
E-mail address: haruka-goto@pola.co.jp (H. Goto)

[1]These authors contributed equally to this work.

13 December 2012

http://dx.doi.org/10.1016/j.jdermsci.2013.04.017

Letter to the Editor

Genetic polymorphisms in the *IL22* gene are associated with psoriasis vulgaris in a Japanese population

Keywords:
Genetic polymorphisms; *IL22* gene;
Psoriasis vulgaris; Japanese population

To the Editor,

Psoriasis vulgaris (PsV) is an inflammatory skin disease histologically characterized by epidermal hyperplasia, inflammatory cell infiltration and vascular changes in which T-lymphocytes and associated cytokines play a central role [1]. A dysregulated cutaneous immune response occurs in genetically susceptible individuals and the features of inflammation are characterized by tumor necrosis factor (TNF)-α dependence and exaggerated helper T cell 1 (Th1) and 17 (Th17) activation. Interleukin (IL)-22 is an IL-10 family cytokine member produced by Th17 cells and plays a role in the promotion of inflammation and tissue repair at barrier surfaces [2]. IL-22 is required for Th17 cell-mediated pathology in a mouse model of psoriasis-like skin inflammation [3], and circulating IL-22 levels are significantly higher in psoriatic patients than in normal subjects [4,5]. Atopic dermatitis (AD) is a chronic, relapsing inflammatory skin disease that is basically considered to be a Th-2 type disease. However, a recent study suggests a possible role of Th17 cells in AD [6]. The study has shown that the number of Th17 cells is increased in the peripheral blood and acute lesional skin of AD and that IL-17 and IL-22 synergistically enhance the production of IL-8 from keratinocytes [6]. Since there are few genetic studies of the polymorphisms of *IL22* in populations of Asian and European ancestry, we conducted association studies to assess whether *IL22* gene variants contribute to the susceptibility to PsV or AD in a Japanese population.

We recruited a total of 236 patients with PsV (mean age 53, 11–85 years, male:female ratio = 1.0:2.8), and all subjects were diagnosed by clinical and histopathological findings. A total of 916 patients with AD (mean age 30, 3–77 years, male:female ratio = 1.0:2.2) and 844 controls (mean age 50, 20–75 years, male:female ratio = 1.0:1.3) were recruited as described [7]. Patients with AD were diagnosed according to the criteria of Hanifin and Rajka, and control subjects were never diagnosed with AD or PsV. All individuals were unrelated Japanese and gave written informed consent to participate in the study. The study was approved by the ethical committees at the Institute of Physical and Chemical Research (RIKEN), the University of Tokyo and the Jikei University School of Medicine. Genomic DNA was prepared in accordance with standard protocols.

We resequenced the *IL22* gene regions with genomic DNA from 36 individuals and identified a total of 32 polymorphisms (Table 1). We next examined the linkage disequilibrium (LD) between identified SNPs (Fig. S1). Pairwise LD coefficients D' and r^2 were calculated among the 24 SNPs with minor allele frequencies (MAF) of greater than 5% using Haploview 4.2 (http://www.broad.mit.edu/mpg/haploview/). We selected a total of 11 tag SNPs for association studies using tagger in Haploview 4.2, and the 11 tag

Table 1
Frequencies of polymorphisms of the *IL22* gene in a Japanese population.

	SNP[a]	Allele	Location	MAF[b]	NCBI[c]
1	−2479	T/C	5′-Flanking region	0.319	rs57947370
2	−2378	C/T	5′-Flanking region	0.278	rs11177135
3	−2375	T/C	5′-Flanking region	0.014	rs77156535
4	−2161	G/A	5′-Flanking region	0.319	rs7139027
5	−1905	A/G	5′-Flanking region	0.278	rs2227472
6	−1810	G/A	5′-Flanking region	0.319	rs2227473[d]
7	−1588	T/A	5′-Flanking region	0.292	rs2227476[d]
8	−1536	C/T	5′-Flanking region	0.028	rs2227477
9	−1394	T/C	5′-Flanking region	0.431	rs2227478[d]
10	−1114	C/T	5′-Flanking region	0.111	rs2227480
11	−1113	C/T	5′-Flanking region	0.278	rs2227481
12	−1089	AT/del	5′-Flanking region	0.000	rs35774195
13	−1075	AT repeat	5′-Flanking region	0.000	rs10699698
14	−948	T/A	5′-Flanking region	0.292	rs2227483
15	−701	C/T	5′-Flanking region	0.111	rs2227484[d]
16	−485	C/T	5′-Flanking region	0.278	rs2227485[d]
17	−201	A/G	5′-Flanking region	0.014	rs141972126
18	393	T/A	Intron 1	0.264	rs17224704[d]
19	708	A/G	Intron 2	0.278	rs2227491
20	1254	A/C	Intron 3	0.375	rs2046068[d]
21	1366	G/T	Intron 3	0.028	rs3782552
22	1945	G/C	Intron 4	0.014	
23	2178	G/C	Intron 4	0.361	rs1179251[d]
24	2385	T/C	Intron 4	0.097	rs1179250[d]
25	2449	C/A	Intron 4	0.097	rs1179249
26	2611	T/A	Intron 4	0.278	rs1012356
27	3270	C/A	Intron 4	0.278	rs2227501
28	3531	A/G	Intron 4	0.278	rs2227503
29	3635	T/C	Intron 4	0.014	rs976748
30	5301	A/T	3′-Flanking region	0.097	rs2227508[d]
31	5433	CT/del	3′-Flanking region	0.014	
32	5697	A/T	3′-Flanking region	0.444	rs1182844[d]

[a] Numbering according to the genomic sequence of IL-22 (NC_000012.11). Position 1 is the A of the initiation codon.
[b] MAF (minor allele frequencies) in the screening population ($N = 36$).
[c] NCBI, number from the dbSNP of NCBI (http://www.ncbi.nlm.nih.gov/SNP/).
[d] SNPs were genotyped in this study. Genotyping of the 11 SNPs in IL-22 were performed by the TaqMan™ allele-specific amplification (TaqMan-ASA) method (Applied Biosystems) and multiplex-PCR based Invader assay (Third Wave Technologies).

Table 2
Summary of association results for the *IL22* gene.

dbSNP allele 1/2 position	Subject	Genotype			Total	Frequency			MAF	1 vs. 2 alleles		
		11	12	22		11	12	22		*P* value	OR	95% CI
rs2227473	PsV	130	94	10	234	0.556	0.402	0.043	0.244	0.0095	1.38	1.08–1.76
G/A	AD	604	274	32	910	0.664	0.301	0.035	0.186	0.79	1.02	0.86–1.21
−1810	Control	550	262	28	840	0.655	0.312	0.033	0.189			
rs2227476	PsV	136	88	9	233	0.584	0.378	0.039	0.227	0.0051	1.43	1.11–1.84
T/A	AD	633	256	26	915	0.692	0.280	0.028	0.168	0.84	1.02	0.85–1.21
−1588	Control	578	242	23	843	0.686	0.287	0.027	0.171			
rs2227478	PsV	98	101	37	236	0.415	0.428	0.157	0.371	0.00014	1.51	1.22–1.88
T/C	AD	470	363	82	915	0.514	0.397	0.090	0.288	0.60	1.04	0.90–1.20
−1394	Control	429	353	59	841	0.510	0.420	0.070	0.280			
rs2227484	PsV	187	41	7	235	0.796	0.174	0.030	0.117	0.30	1.18	0.86–1.64
C/T	AD	735	166	12	913	0.805	0.182	0.013	0.104	0.74	1.04	0.83–1.29
−701	Control	674	154	7	835	0.807	0.184	0.008	0.101			
rs2227485	PsV	92	105	38	235	0.391	0.447	0.162	0.385	0.024	1.27	1.03–1.57
C/T	AD	289	447	179	915	0.316	0.489	0.196	0.440	0.84	1.01	0.89–1.16
−485	Control	258	418	163	839	0.308	0.498	0.194	0.443			
rs17224704	PsV	146	82	7	235	0.621	0.349	0.030	0.204	0.023	1.35	1.04–1.75
T/A	AD	653	242	18	913	0.715	0.265	0.020	0.152	0.54	1.06	0.88–1.27
393	Control	595	225	22	842	0.707	0.267	0.026	0.160			
rs2046068	PsV	104	102	26	232	0.448	0.440	0.112	0.332	0.0018	1.42	1.14–1.78
A/C	AD	501	342	71	914	0.548	0.374	0.078	0.265	0.69	1.03	0.89–1.20
1254	Control	458	329	53	840	0.545	0.392	0.063	0.259			
rs1179251	PsV	124	85	26	235	0.528	0.362	0.111	0.291	0.54	1.07	0.86–1.34
G/C	AD	454	372	90	916	0.496	0.406	0.098	0.301	0.75	1.02	0.89–1.18
2178	Control	408	351	82	841	0.485	0.417	0.098	0.306			
rs1179250	PsV	134	84	17	235	0.570	0.357	0.072	0.251	0.23	1.15	0.91–1.46
T/C	AD	487	354	74	915	0.532	0.387	0.081	0.274	0.77	1.02	0.88–1.19
2385	Control	439	338	66	843	0.521	0.401	0.078	0.279			
rs2227508	PsV	187	41	7	235	0.796	0.174	0.030	0.117	0.11	1.31	0.94–1.81
T/A	AD	737	162	12	911	0.809	0.178	0.013	0.102	0.32	1.12	0.90–1.40
5301	Control	694	141	7	842	0.824	0.167	0.008	0.092			
rs1182844	PsV	83	108	43	234	0.355	0.462	0.184	0.415	0.54	1.07	0.87–1.31
A/T	AD	327	428	158	913	0.358	0.469	0.173	0.407	0.61	1.04	0.91–1.19
5697	Control	310	391	140	841	0.369	0.465	0.166	0.399			

SNPs captured 24 of the 24 alleles with $r^2 > 0.92$. We genotyped the 11 SNPs in *IL22* gene by the TaqMan® SNP Genotyping Assays (Life Technologies).

Supplementary data associated with this article can be found, in the online version, at http://dx.doi.org/10.1016/j.jdermsci.2013.04.002.

The results for genotype frequencies of the 11 tag SNPs in the case and control group are shown in Table 2. All 11 SNPs were in Hardy–Weinberg equilibrium, and we then compared differences in the allele frequencies by using a contingency χ^2 test. Odds ratios (ORs) with 95 percent confidence intervals (95% CI) were calculated. We applied Bonferroni corrections, the multiplication of *P* values by 11, the number of tag SNPs. In the association study, corrected *P* values of less than 0.05 were judged to be significant.

We identified significant associations between *IL22* gene variants and PsV under the allelic model (rs2227478; corrected $P = 0.0015$; OR = 1.51, rs2046068; corrected $P = 0.020$; OR = 1.42) (Table 2). Weger et al. evaluated a total of 10 common polymorphisms of the *IL22* gene in an Austrian population and reported no association between the variants and chronic plaque psoriasis [8]. Recent genome-wide association studies (GWASs) of PsV revealed a total of 36 psoriasis-associated regions in individuals of European ancestry, and the regions encode several proteins engaged in the TNF, IL-23 and IL-17 signaling pathways [9]. However, the *IL22* locus did not contain the susceptible regions identified by European GWASs. Since heterogeneous association signals are often seen among different ethnic populations, further genetic studies using Asian populations seem to be needed for further focusing attention of polymorphisms of the *IL22* gene in this disease. Although a validation study in an independent population is needed, our findings imply that *IL22* variants play a role in the pathogenesis of PsV in the Japanese population.

A number of features shared by AD and PsV including a Th17 cell pathway and common gene loci, were reported [10], but we did not find a significant association in this study between *IL22* SNPs and susceptibility to AD ($P = 0.32$–0.84) (Table 2). Since a recent study has shown a role of Th17 cells in exacerbation of AD [6], genetic variants of *IL22* might influence the exacerbation of the disease rather than susceptibility to it.

In summary, our data suggested important genetic influences of the polymorphisms in *IL22* on the susceptibility to PsV but not to AD in the Japanese population. Higher concentrations of IL-22 are observed in the peripheral blood and tissues of patients with PsV [2,4,5], and expression of IL-22 and IL-22-regulated genes in keratinocytes is reduced by antipsoriatic therapies [4]. Further evaluation of the clinical significance of the susceptible *IL22* gene variants would help better understand the etiology of PsV.

Acknowledgments

We thank all the individuals who participated in the study. We also thank M.T. Shimizu, H. Sekiguchi, A.I. Jodo, N. Kawaraichi and

the technical staff of the Center for Genomic Medicine for providing technical assistance and K. Barrymore for proofreading this manuscript. This work was supported by Health Science Research Grants from the Ministry of Health, Welfare and Labor of Japan and the Ministry of Education, Culture, Sports, Science and Technology, Japan.

References

[1] Kaplan DH, Barker J. Psoriasis. N Engl J Med 2009;361:496–509.
[2] Sonnenberg GF, Fouser LA, Artis D. Border patrol: regulation of immunity, inflammation and tissue homeostasis at barrier surfaces by IL-22. Nat Immunol 2011;12:383–90.
[3] Ma HL, Liang S, Li J, Napierata L, Brown T, Benoit S, et al. IL-22 is required for Th17 cell-mediated pathology in a mouse model of psoriasis-like skin inflammation. J Clin Invest 2008;118:597–607.
[4] Wolk K, Witte E, Wallace E, Döcke WD, Kunz S, Asadullah K, et al. IL-22 regulates the expression of genes responsible for antimicrobial defense, cellular differentiation, and mobility in keratinocytes: a potential role in psoriasis. Eur J Immunol 2006;36:1309–23.
[5] Boniface K, Guignouard E, Pedretti N, Garcia M, Delwail A, Bernard FX, et al. A role for T cell-derived interleukin 22 in psoriatic skin inflammation. Clin Exp Immunol 2007;150:407–15.
[6] Koga C, Kabashima K, Shiraishi N, Kobayashi M, Tokura Y. Possible pathogenic role of Th17 cells for atopic dermatitis. J Invest Dermatol 2008; 128:2625–30.
[7] Shimizu M, Matsuda A, Yanagisawa K, Hirota T, Ahahoshi M, Inomata N, et al. Functional SNPs in the distal promoter of the ST2 gene are associated with atopic dermatitis. Hum Mol Genet 2005;14:2919–27.
[8] Weger W, Hofer A, Wolf P, El-Shabrawi Y, Renner W, Kerl H, et al. Common polymorphisms in the interleukin-22 gene are not associated with chronic plaque psoriasis. Exp Dermatol 2009;18:796–8.
[9] Tsoi LC, Spain SL, Knight J, Ellinghaus E, Stuart PE, Capon F, et al. Identification of 15 new psoriasis susceptibility loci highlights the role of innate immunity. Nat Genet 2012;44:1341–8.
[10] Wilsmann-Theis D, Hagemann T, Jordan J, Bieber T, Novak N. Facing psoriasis and atopic dermatitis: are there more similarities or more differences? Eur J Dermatol 2008;18:172–80.

Hidehisa Saeki[a,1,*], Tomomitsu Hirota[b,1], Hidemi Nakagawa[a], Yuichiro Tsunemi[c], Toyoaki Kato[d], Sayaka Shibata[d], Makoto Sugaya[d], Shinichi Sato[d], Satoru Doi[e], Akihiko Miyatake[f], Kouji Ebe[g], Emiko Noguchi[h], Tamotsu Ebihara[i], Masayuki Amagai[i], Hitokazu Esaki[j], Satoshi Takeuchi[j], Masutaka Furue[j], Yusuke Nakamura[k], Mayumi Tamari[b]

[a]*Department of Dermatology, The Jikei University School of Medicine, Japan*; [b]*Laboratory for Respiratory Diseases, Center for Genomic Medicine, RIKEN, Japan*; [c]*Department of Dermatology, Tokyo Women's Medical University, Japan*; [d]*Department of Dermatology, Faculty of Medicine, University of Tokyo, Japan*; [e]*Osaka Prefectual Medical Center for Respiratory and Allergic Diseases, Japan*; [f]*Miyatake Asthma Clinic, Japan*; [g]*Takao Hospital, Japan*; [h]*Graduate School of Comprehensive Human Sciences, University of Tsukuba, Japan*; [i]*Department of Dermatology, Keio University School of Medicine, Japan*; [j]*Department of Dermatology, Graduate School of Medical Sciences, Kyushu University, Japan*; [k]*Institute of Medical Science, The University of Tokyo, Japan*

*Corresponding author at: Department of Dermatology, The Jikei University School of Meicine, 3-25-8, Nishishimbashi, Minato-ku, Tokyo 105-8461, Japan.
Tel.: +81 3 3433 1111; fax: +81 3 5401 0125
E-mail address: saeki-der@jikei.ac.jp (H. Saeki)

[1]These authors contributed equally to this article.

1 March 2013

http://dx.doi.org/10.1016/j.jdermsci.2013.04.002

Letter to the Editor

HLA-B*58:01 strongly associates with allopurinol-induced adverse drug reactions in a Japanese sample population

To the Editor,

Allopurinol, an inhibitor of xanthine oxidase, is widely used for the treatment of hyperuricemia associated with chronic gout, acute uric acid nephropathy, recurrent uric acid stone formation, certain enzyme/blood disorders, and cancer chemotherapy. It has been shown that severe cutaneous adverse drug reactions (ADRs) caused by allopurinol were strongly associated with HLA-B*58:01 in a Han Chinese sample population [1]. Odds ratio (OR) for the association of HLA-B*58:01 with allopurinol-induced severe cutaneous ADR in this population was 580.3 and 95% CI was 34.4–9780.9. Although the relationship between HLA-B*58:01 and allopurinol-induced Stevens–Johnson syndrome (SJS) and toxic epidermal necrolysis (TEN) has subsequently been studied in European and Japanese patients, the association was much weaker than that reported in Han Chinese patients [2,3]. The association study in Japanese patients was examined in only a limited number of allopurinol-induced ADR cases. We therefore conducted a case-controlled study to determine HLA types associated with allopurinol-induced ADR in a Japanese sample population.

All patients were recruited from Shimane University Hospital between 2010 and 2012. These included 7 patients with allopurinol-induced ADR (3 patients with SJS and 4 patients with erythema exudativum multiforme (EEM)) and 25 patients who had been receiving allopurinol for more than 3 months without drug eruption. Diagnoses of SJS were made according to the diagnostic criteria established by Roujeau [4]. Allopurinol-induced ADR was diagnosed using medical histories, indicating that symptoms occurred within 3 months of starting allopurinol administration, and the symptoms resolved upon the withdrawal of allopurinol. If the patients were given other drugs, in addition to allopurinol, 3 months prior to the appearance of symptoms, a drug-induced lymphocyte stimulation test and a patch test were performed with allopurinol/oxypurinol. Allopurinol-induced ADRs were diagnosed by the single medication of allopurinol in 4 of the 7 patients (No. 1, 3, 4, 7), by the positive allopurinol-induced lymphocyte stimulation test in 2 of the 7 patients (No. 2, 6), and by the positive patch test with allopurinol in the patient No. 5. The indication for which drug had been prescribed was the level of hyperuricemia detected in all the patients. All patients were interviewed by investigators regarding the histories of their biological parents and grandparents, and were confirmed as being ethnically Japanese. This study was approved by the ethics committee of Shimane University Faculty of Medicine (approval no. 221).

Low-resolution HLA typing with DNA extracted from peripheral blood was performed using the reverse sequence-specific oligonucleotide with polymerase chain reaction (PCR-rSSO) method [5]. High-resolution HLA-B genotyping was determined using the polymerase chain reaction-sequence based typing (PCR-SBT) method [5]. Statistical analysis of the differences in each allele frequency among patients with ADR and control subjects was performed by Fisher's exact test. The strength of association was estimated by calculating the OR. The OR was determined using Haldane's modification, which adds 0.5 to all cells to accommodate

Case Reports in Clinical Medicine, 2014, 3, 639-643
Published Online December 2014 in SciRes. http://www.scirp.org/journal/crcm
http://dx.doi.org/10.4236/crcm.2014.312136

Scientific Research

Necrobiosis Lipoidica in the Absence of Diabetes Mellitus: A Case Report and an Analysis of 116 Japanese Cases

Ayumi Korekawaka, Koji Nakajima, Hajime Nakano, Daisuke Sawamura*

Department of Dermatology, Hirosaki University Graduate School of Medicine, Hirosaki, Japan
Email: *m981027@cc.hirosaki-u.ac.jp

Received 23 October 2014; revised 22 November 2014; accepted 3 December 2014

Abstract

A 60-year-old Japanese woman was referred to our hospital for yellow-brown plaques accompanied by ulceration on her left lower leg. Her medical history included neither diabetes mellitus nor minor trauma. A histopathological examination of the plaques showed necrobiotic changes within the dermal collagen surrounded by granulomas that comprised lymphocytes, histiocytes, and giant cells. The lower dermis revealed fibrotic changes that extended into the subcutaneous tissue. The patient's blood glucose and glycated hemoglobin levels were within the normal ranges. We considered a diagnosis of necrobiosis lipoidica (NL) in the absence of diabetes mellitus. We reviewed 116 cases of NL that were reported in the Japanese medical literature between 1986 and 2014 and found that NL onset was most common in individuals of both sexes ≥ 60 years of age. Previous reports that reviewed NL cases in the Japanese medical literature that were published during the1900s indicated that NL occurs in people ≥ 40 years of age. We suggest that the aging population and increasingly longer life spans have increased the average age of NL onset in Japan. With regard to treatments, there were no effective treatments, but skin grafts were curative. NL treatment is very difficult, especially when ulcers are present; hence, we suggest that further research is needed to determine effective NL treatments.

Keywords

Peripheral Circulatory Disturbance, Ulceration, Trauma, Lower Leg

1. Introduction

Necrobiosis lipoidica (NL) is a rare and benign granulomatous disease that is associated with collagen degeneration and typically affects the lower legs of women. It is characterized by well-defined ulcerated plaques with

*Corresponding author.

How to cite this paper: Korekawaka, A., Nakajima, K., Nakano, H. and Sawamura, D. (2014) Necrobiosis Lipoidica in the Absence of Diabetes Mellitus: A Case Report and an Analysis of 116 Japanese Cases. *Case Reports in Clinical Medicine*, **3**, 639-643. http://dx.doi.org/10.4236/crcm.2014.312136

indurate borders and atrophic centers that often impair patient quality of life when form ulcerations in skin lesions, especially in lower legs.

NL is associated with diabetes mellitus in 80% - 90% of cases. Although its pathogenesis has been discussed in the context of diabetes mellitus, its co-occurrence with peripheral circulatory disturbances and autoimmune disorders has yet to be established. There are no clear specific treatments for NL. Here we describe the case of a Japanese woman who was diagnosed with NL in the absence of diabetes mellitus and report on an analysis of 116 Japanese NL cases.

2. Case Report

A 60-year-old Japanese woman was referred to our hospital in June 2014 with a 2-year history of yellow-brown plaques on her lower left leg. The plaques had gradually worsened over time. The lesions were irregularly shaped, well-circumscribed, atrophic yellow-brown plaques, and the largest was accompanied by a small ulcer (Figure 1(a), Figure 1(b)). There was no leg edema, associated pain, or itching as well as no varices. Her medical history did not include diabetes mellitus, metabolic disorders, or minor trauma. She had stitched clothing for many years and stood for long periods of time as she worked. The patient's lesions were clinically diagnosed as NL, and we performed a skin biopsy.

A histopathological examination showed necrobiotic changes within the dermal collagen that were surrounded by granulomas that comprised lymphocytes, histiocytes, and giant cells (Figures 1(c)-(e)). The lower dermis revealed fibrotic changes that extended into the subcutaneous tissue. The blood vessels in that region did not show any particularly abnormal changes. The epidermis was mildly atrophic. Laboratory test results, including blood glucose and glycated hemoglobin levels, were within the normal ranges. A 75-goral glucose tolerance test produced normal results.

We treated the patient with topical corticosteroids but saw no noticeable improvement. Given the diagnosis of NL in the absence of diabetes mellitus, we administered topical therapy that comprised alprostadil alfadex ointment (0.003%). By 2 months after the treatment initiation, the lesions had decreased in size.

3. Discussion

NL is an idiopathic chronic granulomatous inflammatory disorder characterized by collagen degeneration, granuloma formation, fat deposition, and thickening of the blood vessel walls. NL is often associated with diabetes mellitus, thyroid dysfunction, sarcoidosis, rheumatoid arthritis, inflammatory bowel disease, and peripheral circulatory disturbances, and most cases of NL are idiopathic [1]. The most commonly affected regions are the pretibial areas.

We reviewed 116 NL cases that were reported in the Japanese medical literature between 1986 and 2014 including the present case. Thirteen menaged 21 - 75 years and 103 women aged 31 - 86 years were evaluated with regard to their epidemiological data, the presence of ulcers, lesion, laboratory test results, treatment provided, and treatmenteffects. NL was considerably more frequent in women (89%) (Figure 2(a)). NL onset was most common when people of both sexes were aged ≥ 60 years, and the average age of NL onset was 55.5 years in women and 56.4 years in men (Figure 2(b), Figure 2(c)). Reports from countries other than Japan indicated that NL occurs during the third or fourth decades of life in both sexes [2]-[4] Previous reports that reviewed NL cases in the Japanese medical literature published during the 1900s indicated that the average age range at NL onset was the 40s in both sexes [5]. However, reports that reviewed NL cases in the Japanese medical literature published during the 2000s indicated that the average age at NL onset was ≥50 years in both sexes [6] [7]. We suggest that the aging population and extended lifes pans have increased the average age of NL onset in Japan.

The incidence of diabetes mellitus among people with NL is reportedly 77% for men and 30% for women. In 48% of men, NL lesions were found in areas other than the pretibial regions, including the forearms, chest, abdomen, thighs, fingers, scrotum, and penis. In contrast, only 8% of women had lesions in atypical locations, including the face, back, groin, abdomen, and chest (Figure 2(d)). We found that the presence of diabetes mellitus with NL and atypical lesion locations occurred predominantly in men.

Of the patients whose cases were reviewed, ulceration of the NL lesions occurred in 14% and trauma preceded NL in 23% of men and in 19% of women. Although 9.4% of all of cases reviewed had neither metabolic disorders nor trauma, they did have histories that were indicative of circulatory disturbances, which included

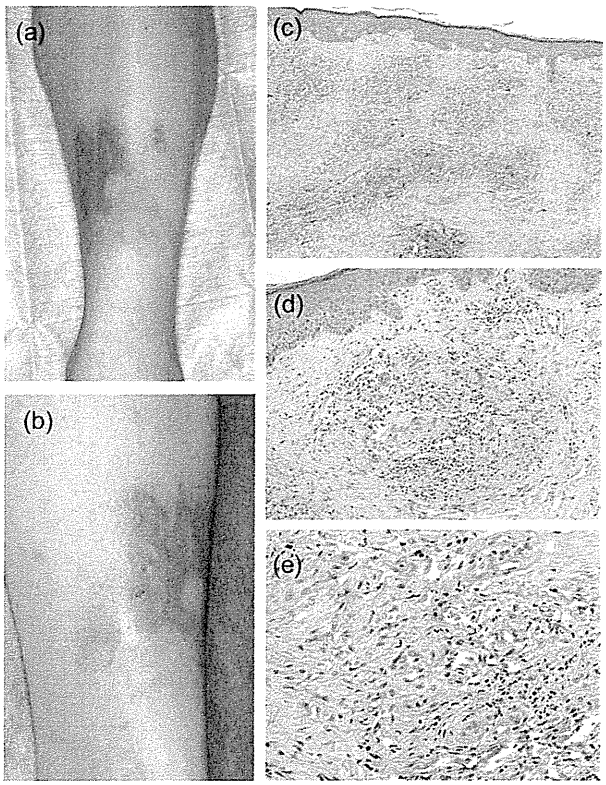

Figure 1. Clinical manifestations and histopathological findings. (a) (b) Irregularly shaped, well-circumscribed, atrophic yellow-brown necrobiosis lipoidica plaques, one of which is accompanied by a small ulcer on the patient's lower left leg; (c)-(e) Necrobiotic changes within the dermal collagen that are surrounded by granulomasthatcomprise lymphocytes, histiocytes, and giant cells. Fibrotic changes that are apparent in the lower dermis extend into the subcutaneous tissue (hematoxylin and eosin, Figure 1(c) 40×, Figure 1(b) 100×, and Figure 1(e) 400×).

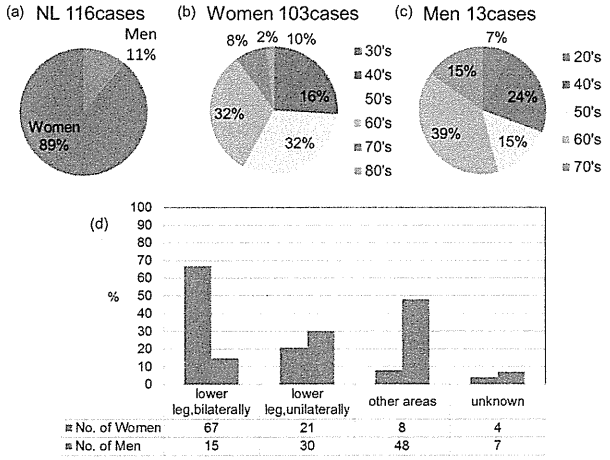

Figure 2. (a)-(c) Epidemiological data and lesion locations. Necrobiosis lipoidica (NL) is considerably more frequent in women and the onset is most common when people of both sexes are ≥60 yearsof age; (d) NL lesions are found in areas other than the pretibial regions, including the forearms, chest, abdomen, thighs, fingers, scrotum, and penis in 48% of men.

standing for long periods of time while working, lymph edema of the affected parts, postoperative effects, and varices. Although there was no history of metabolic disorders, minor trauma, edema, or varices and there were no histopathological findings associated with the blood vessels in our case, the patient had worked for many years stitching clothing and had stood for long periods of time while she worked. We propose that her work had

induced peripheral circulatory disturbances that triggered collagen degeneration.

Topical corticosteroids, the mainstay of NL treatment, were used in 25 cases. Aspirin (900 - 1000 mg/day) and dipyridamole (150 - 225 mg/day) given in combination, oral corticosteroids (20 - 30 mg/day), fludroxycortide tape, and herbal preparations including modified Merry Life Powder, which comprised a rhubarb and moutan bark decoction, were effective, and operations comprising excisions or skin grafts were curative (Table 1). Many cases were given several different treatment types. Topical tacrolimus was used to treat three patients with

Table 1. Treatment options for necrobiosis lipoidica and treatment outcomes.

Treatment	No. of cases	No. of effective cases
No. of methods: one		
Topical corticosteroids	25	11
Fludroxycortide tape (4 μg/cm^2)	3	2
Moisturizer	2	0
Anti-ulcer agents	3	3
Tacrolimus	2	1
Oral corticosteroids (20 - 30 mg/day)	7	6
Tranilast	2	1
Tocopherol nicotinate	3	2
Aspirin	4	2
Herbal preparations	2	2
Ethyl icosapentate	1	1
Local injection corticosteroids	3	1
Others compression therapy	1	1
PDT (photodynamic therapy)	1	1
PUVA (psoralen plus ultraviolet)	2	1
operation (excision or skin graft)	5	5
No. of methods: two		
Topical only corticosteroids plus moisturizer	4	2
Corticosteroids plus anti-ulcer agents	2	1
Tacrolimus plus corticosteroids	1	0
Oral plus topical tranilast (oral) plus corticosteroids(topical)	1	1
Aspirin (oral) plus corticosteroids(topical)	1	0
Oral only tocopherol nicotinate plus aspirin	1	1
Aspirin (900 - 1000 mg/day) and dipyridamole (150 - 225 mg/day)	5	5
Others losing weight plus topical corticosteroids	1	0
Losing weight plus maintaining adequate glucose control	2	1
Compression therapy plus topical corticosteroids	1	0
PUVA plus compression therapy	1	0
PUVA plus topical corticosteroids	1	1
Near-infrared light treatment plus topical 0.003% alprostadil alfadex ointment	1	1
No. of methods: three		
Compression therapy plus topical corticosteroids plus sarpogrelate hydrochloride	1	1
Oral tranilast plus topical corticosteroids plus compression therapy	1	1
PUVA plus compression therapy plus corticosteroid local injection	1	1
Oral corticosteroids (30 mg/day) plus operation (excision or skin graft) plus corticosteroidlocal injection	1	1
No. of methods:more than three		
Oral clarithromycin plus oral tranilast plus topical corticosteroids plus topical anti-ulcer agents plus topical 0.003% alprostadil alfadex ointment	1	1
Methods: unknown	23	

NL, but no notable improvements were observed. While operative procedures seem to heal NL completely, there is a risk of relapse because of vascular damage and koebnerization; hence, we should be careful when making treatment decisions.

4. Conclusion

Treating NL is very difficult, especially cases of ulcerated NL, and squamous cell carcinomais often associated with ulcerated NL [8]. We suggest the need for further research to determine effective treatments for NL.

Conflict of Interest Statement

The authors declare no conflicts of interest.

References

[1] Chung, C.G., Rosengrant, A., Helm, K.F. and Shupp, D.L. (2014) Necrobiosis Lipoidica Occurring in a Patient with Rheumatoid Arthritis on Concurrent Tumor Necrosis Factor-α Inhibitor Therapy. *International Journal of Dermatology*. http://dx.doi.org/10.1111/ijd.12309

[2] Reid, S.D., Ladizinski, B., Lee, K., Baibergenova, A. and Alavi, A. (2013) Update on Necrobiosis Lipoidica: A Review of Etiology, Diagnosis, and Treatment Options. *Journal of the American Academy of Dermatology*, **69**, 783-791. http://dx.doi.org/10.1016/j.jaad.2013.05.034

[3] Erfurt-Berge, C., Seitz, A.T., Rehse, C., Wollina, U., Schwede, K. and Renner, R. (2012) Update on Clinical and Laboratory Features in Necrobiosis Lipoidica: A Retrospective Multicentre Study of 52 Patients. *European Journal of Dermatology*, **22**, 770-775.

[4] Pătraşcu, V., Giurcă, C., Ciurea, R.N., Georgescu, C.C. and Ciurea, M.E. (2014) Ulcerated Necrobiosis Lipoidica to a Teenager with Diabetes Mellitus and Obesity. *Romanian Journal of Morphology and Embryology*, **55**, 171-176.

[5] Masatoshi, A., Kazunori, O., Osamu, I., Yoshiki, M., Toshiya, I. and Kyohei, S. (1999) Twocases of Necrobiosis Lipoidica—Its Relationships with Diabetes Mellitus and Preceding Trauma in the Japanese Patients. *Rinsho Derma* (*Tokyo*), **53**, 529-532.

[6] Mariko, Y., Yasuhiko, M., Takekuni, N., Shinichiro, Y., Takashi, H. and Kenichiro, I. (2006) A Case of Necrobiosis Lipoidica without Diabetes Mellitus. *Rinsho Derma* (*Tokyo*), **60**, 1020-1022.

[7] Misaki, O., Yoshihiro, S., Yuichi, T. and Seiichi, I. (2011) A Case of Necrobiosis Lipoidica Associated with Venous Insufficiency of Both Legs. *Rinsho Derma* (*Tokyo*), **65**, 497-500.

[8] Uva, L., Freitas, J., Soares de Almeida, L., Vasques, H., Moura, C. and Miguel, D. (2013) Squamous Cell Carcinoma Arising in Ulcerated Necrobiosis Lipoidica Diabeticorum. *International Wound Journal*. http://dx.doi.org/10.1111/iwj.12206

Phytochemistry 102 (2014) 169–181

Contents lists available at ScienceDirect

Phytochemistry

journal homepage: www.elsevier.com/locate/phytochem

Hepatoprotective triterpenes from traditional Tibetan medicine *Potentilla anserina*

Toshio Morikawa, Kiyofumi Ninomiya, Katsuya Imura, Takahiro Yamaguchi, Yoshinori Akagi, Masayuki Yoshikawa, Takao Hayakawa, Osamu Muraoka *

Pharmaceutical Research and Technology Institute, Kinki University, 3-4-1 Kowakae, Higashi-osaka, Osaka 577-8502, Japan

ARTICLE INFO

Article history:
Received 4 April 2013
Received in revised form 30 January 2014
Available online 31 March 2014

Keywords:
Potentilla anserina
Rosaceae
Hepatoprotective activity
Potentillanoside
Ursane-type triterpene 28-*O*-monoglucopyranosyl ester
Traditional Tibetan medicine

ABSTRACT

A methanol extract from the tuberous roots of *Potentilla anserina* (Rosaceae) exhibited hepatoprotective effects against D-galactosamine (D-GalN)/lipopolysaccharide-induced liver injuries in mice. Six triterpene 28-*O*-monoglucopyranosyl esters, potentillanosides A–F, were isolated from the extract along with 32 known compounds, including 15 triterpenes. The structures of potentillanosides A–F were determined on the basis of spectroscopic properties and chemical evidence. Four ursane-type triterpene 28-*O*-monoglycosyl esters, potentillanoside A (IC_{50} = 46.7 μM), 28-*O*-β-D-glucopyranosyl pomolic acid (IC_{50} = 9.5 - μM), rosamutin (IC_{50} = 35.5 μM), and kaji-ichigoside F1 (IC_{50} = 14.1 μM), inhibited D-GalN-induced cytotoxicity in primary cultured mouse hepatocytes. Among these four triterpenes, potentillanoside A, rosamutin, and kaji-ichigoside F1 exhibited *in vivo* hepatoprotective effects at doses of 50–100 mg/kg, p.o. The mode of action was ascribable to the reduction in cytotoxicity caused by D-GalN.

Introduction

The plant *Potentilla anserina* L. (Rosaceae) is widely distributed in the western areas of China, particularly in the Qinghai-Tibetan Plateau (Wang et al., 2010; Xia and You, 2011). In traditional Tibetan medicine, roots of this plant have been used to treat malnutrition, anemia, diarrhea, and haemorrhage (Chen et al., 2010). Several chemical constituents of this plant, such as tannins (Schimmer and Lindenbaum, 1995), flavan-3-ols and flavonoids (Kombal and Glasl, 1995), triterpenes (Chu et al., 2008; Li et al., 2003), triterpene glycosides (Zhao et al., 2008), polysaccharides (Chen et al., 2010; Wang et al., 2010), and amino acids (Xia and You, 2011) have been reported. In addition, biological activities such as antimutagenic (Schimmer and Lindenbaum, 1995), anti-hepatitis B virus (Zhao et al., 2008), and immunomodulatory activities (Chen et al., 2010) of the extracts and/or constituents have been reported. During our studies on medicinal herbs in Tibet and Xinjiang autonomous regions in China, such as *Cistanche tubulosa* (Morikawa et al., 2010a,b; Pan et al., 2010; Xie et al., 2006; Yoshikawa et al., 2006), *Punica granatum* (Xie et al., 2008), and *Poacynum hendersonii* (Morikawa et al., 2012), a methanol extract of the tuberous roots of *P. anserina* was found to have a protective effect against liver injuries induced by D-galactosamine (D-GalN)/lipopolysaccharide (LPS) in mice. From this methanol extract, we have isolated six new triterpene 28-*O*-monoglucopyranosyl esters named potentillanosides A–F (**1**–**6**) along with 32 compounds, including 15 triterpenes (**7**–**21**). This study deals with the isolation and structural elucidation of these new triterpenenes (**1**–**6**) and their hepatoprotective effects and their possible mode of action.

Results and discussion

Effects of P. anserina methanol extract and its fractions on D-GalN/LPS-induced liver injuries in mice

Dried tuberous roots of *P. anserina* were extracted with methanol under conditions of reflux to yield a methanol extract (23.0% from dried material). The methanol extract at a dose of 500 mg/kg, p.o. in mice showed inhibitory effects against an increase in serum levels of aspartate aminotransaminase (sAST) and alanine transaminase (sALT), which are the markers of liver injuries induced by D-GalN/LPS (Table 1). Following this, the methanol extract was partitioned into ethyl acetate (EtOAc)–H_2O mixture (1:1, v/v) to furnish an EtOAc-soluble fraction (0.58%) and an aqueous phase. The latter was subjected to Diaion HP-20 column chromatography (H_2O → MeOH) to yield H_2O- and MeOH-eluted fractions (21.5% and 0.73%, respectively). A bioassay-guided fractionation established that the EtOAc-soluble and MeOH-eluted fractions were active (percentage inhibition at 250 mg/kg, p.o., 95.8% and 85.1%, respectively, for sAST and 97.0% and 99.1%,

* Corresponding author. Tel.: +81 6 6721 2332; fax: +81 6 6729 3577.
E-mail address: muraoka@phar.kindai.ac.jp (O. Muraoka).

http://dx.doi.org/10.1016/j.phytochem.2014.03.002
0031-9422/

spectrum showed absorption bands at 1725, 1686, and 1655 cm^{-1} ascribable to carbonyl, ester carbonyl, and olefin functionalities, and broad bands at 3470 and 1073 cm^{-1} suggestive of a glycoside structure. In the positive-ion FABMS, a quasimolecular ion peak was observed at *m/z* 671 $[M+Na]^+$, and HRFABMS analysis indicated the molecular formula to be $C_{36}H_{56}O_{10}$. The ^1H and ^{13}C NMR spectra (pyridine-d_5, Table 2), which were assigned with the aid of DEPT, ^1H–^1H COSY, HMQC, and HMBC experiments (Fig. S2), showed signals assignable to seven methyls [δ 1.03, 1.16, 1.20, 1.20, 1.37, 1.57 (3H each, all s, H_3-24, 26, 25, 23, 29, 27), 1.06 (3H, d, J = 6.7 Hz, H_3-30)], a methine bearing an oxygen function [δ 4.79 (1H, dd, J = 6.5, 12.4 Hz, H-2)], an olefin [δ 5.51 (1H, dd, J = 3.5, 3.5 Hz, H-12)], and a ester carbonyl group [δ_C 176.9 (C-28)] together with a β-glucopyranosyl part [δ 6.21 (1H, d, J = 8.1 Hz, H-1′)]. The ^1H and ^{13}C NMR spectroscopic properties of the aglycone part were quite similar to those of **13**. Only a group of signals due to the 28-*O*-β-D-glucopyranosyl ester moiety of **13** was lacking in the spectrum of **1**. In the HMBC experiment, a long-range correlation was observed between the anomeric proton of the glucopyranosyl part and the ester carbonyl carbon. The stereostructure was characterized by a nuclear Overhauser enhancement spectroscopy (NOESY) experiment (Fig. S3). The absolute stereostructure of **1** was determined by derivatizing **1** to **10** and **12** using sodium borohydride ($NaBH_4$) as shown in Fig. 2. Acid hydrolysis of **1** with 5% aqueous H_2SO_4–1,4-dioxane (1:1, v/v) liberated D-glucose, which was identified by HPLC analysis (Morikawa et al., 2010a,b). On the basis of this evidence, the absolute stereostructure of potentilllanoside A was determined as 2α,19α-dihydroxy-3-oxours-12-en-28-oic acid 28-*O*-β-D-glucopyranosyl ester (**1**).

Potentillanoside B (**2**) was obtained as an amorphous powder. Its molecular formula, $C_{36}H_{56}O_{10}$, was found to be the same as that of **1** by HRFABMS measurement. The ^1H and ^{13}C NMR (Table 2) spectroscopic properties were also quite similar to those of 2-oxopomolic aicd 28-*O*-β-D-glucopyranosyl ester (**15**) (Table S1), except for signals due to the A ring part of the aglycone [δ 2.31, 2.97 (1H each, both d, J = 12.4 Hz, H_2-1), 3.92 (1H, s, H-3); δ_C 51.6 (C-1), 213.3 (C-2), 83.1 (C-3)]. The connectivities of the hydroxy and carbonyl moieties in the A ring of the aglycone were characterized on the basis of the HMBC spectrum, in which long-range correlations were observed between: H_2-1 and C-2/C-3/C-10 (δ_C 42.8); H-3 and C-1/C-2/C-4 (δ_C 42.3); and H_3-23 [δ 1.22 (3H, s)]/H_3-24 [δ 0.96 (3H, s)] and C-3/C-4/C-5 (δ_C 50.3). Reduction of **2** with $NaBH_4$ yielded **12**

Table 2
^1H and ^{13}C NMR spectroscopic data (pyridine-d_5) of **1** and **2**.

	1		**2**	
Position	δ_H	δ_C	δ_H	δ_C
1	1.35 (m)	50.2	2.31 (d, 12.4)	51.6
	2.48 (dd, 6.5, 12.5)		2.97 (d, 12.4)	
2	4.79 (dd, 6.5, 12.4)	69.5		213.3
3		216.4	3.92 (s)	83.1
4		48.0		42.3
5	1.23 (br d, *ca.* 12)	69.5	1.99 (dd, 1.6, 12.2)	50.3
6	1.38 (m)	19.6	1.41 (m)	19.5
	1.44 (m)		1.50 (m)	
7	1.43 (m)	33.1	1.48 (m)	33.2
	1.54 (m)		1.72 (m)	
8		40.6		41.1
9	1.83 (dd, 6.9, 10.7)	47.3	2.20 (dd, 6.9, 10.9)	47.8
10		37.9		42.8
11	2.06 (m)	24.1	2.00 (m)	24.0
	2.09 (m)		2.06 (m)	
12	5.51 (dd, 3.5, 3.5)	127.6	5.53 (dd, 3.8, 3.8)	128.0
13		139.3		139.4
14		42.1		42.1
15	1.20 (m)	29.1	1.25 (m)	29.2
	2.40 (ddd, 3.9, 13.1, 13.6)		2.45 (m)	
16	1.98 (m)	26.0	2.03 (m)	26.1
	3.04 (ddd, 3.9, 13.1, 13.3)		3.07 (ddd, 4.3, 13.1, 13.2)	
17		48.5		48.7
18	2.89 (br s)	54.3	2.93 (br s)	54.5
19		72.6		72.7
20	1.35 (m)	42.0	1.39 (m)	42.1
21	1.23 (m)	26.6	1.23 (m)	26.7
	1.96 (m)		1.99 (m)	
22	1.85 (m)	37.6	1.88 (m)	37.6
	2.02 (m)		2.05 (m)	
23	1.20 (3H, s)	25.2	1.22 (3H, s)	27.5
24	1.03 (3H, s)	21.7	0.96 (3H, s)	21.8
25	1.20 (3H, s)	16.0	1.06 (3H, s)	16.9
26	1.16 (3H, s)	17.5	1.16 (3H, s)	17.5
27	1.57 (3H, s)	24.5	1.64 (3H, s)	24.4
28		176.9		176.9
29	1.37 (3H, s)	27.0	1.38 (3H, s)	27.0
30	1.06 (3H, d, 6.7)	16.6	1.06 (3H, d, 7.2)	16.6
28-*O*-Glc				
1′	6.21 (d, 8.1)	95.7	6.27 (d, 8.0)	95.7
2′	4.16 (dd, 7.1, 8.1)	73.9	4.21 (dd, 8.0, 8.6)	74.1
3′	4.24 (dd, 7.1, 8.5)	78.8	4.28 (dd, 8.6, 8.8)	79.0
4′	4.27 (dd, 7.9, 8.5)	71.3	4.32 (dd, 8.8, 9.1)	71.4
5′	4.00 (m)	79.0	4.04 (m)	79.2
6′	4.34 (dd, 4.8, 11.6)	62.4	4.38 (dd, 4.7, 11.9)	62.4
	4.43 (dd, 2.3, 11.6)		4.46 (dd, 2.4, 11.9)	

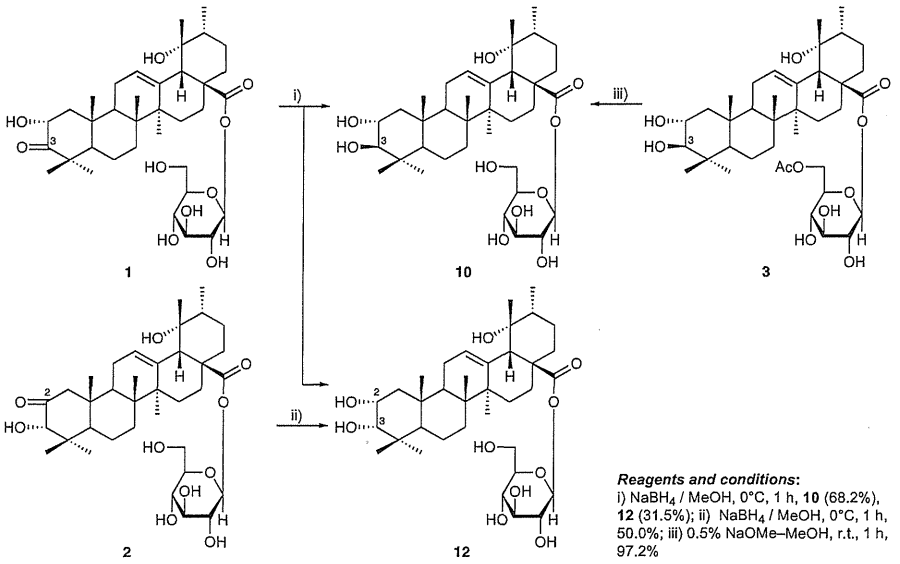

Fig. 2. Absolute stereostructures of **1**–**3**.

(Fig. 2), so that the absolute stereostructure of **2** was determined to be 3α,19α-dihydroxy-2-oxours-12-en-28-oic acid 28-*O*-β-D-glucopyranosyl ester.

Potentillanoside C (**3**) was also obtained as an amorphous powder. Its molecular formula, $C_{38}H_{60}O_{11}$, was determined by a HRFABMS measurement. Its ^1H and ^{13}C NMR (Table 3) spectroscopic properties were quite similar to those of rosamutin (**10**) (Table S2), except for signals due to an acetyl group [δ 1.95 (3H, s); δ_C 170.8 and 20.7]. The connectivity of the acetyl group was clarified by HMBC experiments, which showed a long-range correlation between the 6′-position of the glucopyranosyl part [δ 4.76 (1H, m), 4.86 (1H, dd, J = 1.7, 12.2 Hz)] and the acetyl carbonyl carbon. As shown in Fig. 2, treatment of **3** with 0.5% sodium methoxide (NaOMe)–MeOH provided **10**. Consequently, the stereostructure of **3** was elucidated to be 6′-*O*-acetylrosamutin.

Potentillanoside D (**4**) was obtained as an amorphous powder with a positive optical rotation ($[\alpha]_D^{27}$ + 22.6 in MeOH). Its positive-ion FABMS showed a quasimolecular ion peak at *m*/*z* 703 $[M+H]^+$, and its molecular formula was determined as $C_{36}H_{56}O_{16}$ by HRFABMS measurement. The ^1H and ^{13}C NMR (Table 4) spectra showed signals assignable to seven methyls [δ 1.02 (3H, d, J = 6.6 Hz, H_3-30), 1.26, 1.27, 1.30, 1.55, 1.59, 1.80 (3H each, all s, H_3-25, 26, 29, 23, 24, 27)], an olefin [δ 5.55 (1H, dd, J = 3.5, 3.5 Hz, H-12)], two carboxy and a ester carbonyl groups [δ_C 174.3, 177.0, 182.3 (C-2, 28, 3)] together with a glucopyranosyl part [δ 6.24 (1H, d, J = 8.3 Hz, H-1′)]. As shown in Fig. 3, alkaline hydrolysis of **4** with 5% aqueous potassium hydroxide (KOH)–1,4-dioxane (1:1, v/v) furnished cecropiacic acid (**17**). Finally, the position of the β-D-glucopyranosyl ester was determined on the basis of a HMBC experiment, in which a long-range correlation was observed between H-1′ and C-28. Thus the connected position was unambiguously clarified, and structure **4** was elucidated to be cecropiacic acid 28-*O*-β-D-glucopyranosyl ester. The ^1H and ^{13}C NMR (Table 4) spectroscopic properties of potentillanoside E (**5**) were quite similar to those of **4**, except for signals due to the carbomethoxy group [δ 3.68 (3H, s)]. In the HMBC experiment, a long-range correlation was observed between the carbomethoxy proton and C-3 (δ_C 179.8). As shown in Fig. 3, methylation of **4** and **5** with trimethylsilyldiazomethane ($TMSCHN_2$) gave the common dimethyl ester (**4a**). Thus, the stereostructure of **5** was clarified to be as shown.

Potentillanoside F (**6**) was obtained as an amorphous powder with a positive optical rotation ($[\alpha]_D^{26}$ + 46.9 in MeOH). Its molecular formula, $C_{36}H_{58}O_{11}$, was determined by HRFABMS measurement {*m*/*z* 689.3877 $[M+Na]^+$ (calcd for $C_{36}H_{58}O_{11}Na$, 689.3883)}. The acid hydrolysis of **6** liberated D-glucose, which was identified by HPLC analysis. The ^1H and ^{13}C NMR (Table 5) spectra of **6** showed signals assignable to five methyls [δ 0.98, 1.00, 1.04, 1.12, 1.14 (3H each, all s, H_3-25, 29, 24, 27, 26)], two hydroxymethyls {δ 3.60 (2H, s, H_2-30), [3.70, 4.17 (1H each, both d, J = 10.4 Hz), H_2-23]}, and two methines bearing oxygen functions [δ 4.18 (1H, d, J = 9.4 Hz, H-3), 4.24 (1H, m, H-2)] together with a glucopyranosyl part [δ 6.32 (1H, d, J = 8.1 Hz, H-1′)]. As shown in Fig. 4, a ^1H–^1H COSY experiment indicated the presence of partial structures written in bold lines. In the HMBC experiment, long-range correlations were observed between the following protons and carbons; (H-3 and C-4/C-23/C-24; H-5 and C-4/C-10/C-23/C-24; H_2-7 and C-8; H-9 and C-10; H_2-12 and C-13; H_2-15 and C-14; H_2-16 and C-17; H_2-19 and C-13/C-18/C-20; H_2-21 and C-20; H_2-22 and C-17/C-28; H_2-23 and C-3/C-4/C-5/C-24; H_3-24 and C-3/C-4/C-5/C-23; H_3-25 and C-1/C-5/C-9/C-10; H_3-26 and C-7/C-8/C-9/C-14; H_3-27 and C-8/C-13/C-14; H_3-29 and C-19/C-20/C-21/C-30; H_2-30 and C-19/C-20/C-21/C-29; H-1′ and C-28), respectively. Next, the stereostructure was characterized by a NOESY experiment, which showed NOE correlations between the following proton pairs; {H-1α [δ 1.36 (m)] and H-3; H-2 and H_3-24/H_3-25; H-3 and H-5/H_2-23; H-5 and H-7α [δ 1.54 (m)]/H-9/H_2-23; H-6β [δ 1.37 (m)] and H_3-26; H-9 and H-12α [δ 1.88 (m)]/H_3-27; H-11β [δ 1.28 (m)] and H_3-25; H-12α and H_3-27; H-15β [δ 2.10 (m)] and H_3-26; H-16α [δ 1.61 (m)] and H-22α [δ 1.50 (br dd, J = *ca.* 13, 14 Hz)]/H_3-27/H_3-29; H-22α and H_3-29; H_3-24 and H_3-25; H_3-25 and H_3-26}. Consequently, the structure of **6** was elucidated as 2α,3β,30-trihydroxy-olean-13(18)-en-28-oic acid 28-*O*-β-D-glucopyranosyl ester.

Effects on D-GalN-induced cytotoxicity in primary cultured mouse hepatocytes

D-GalN/LPS-induced liver injuries are known to develop through immunological responses (Freudenberg and Galanos, 1991) that progress *via* two steps. First, expression of inhibitors against apoptosis (IAPs) is inhibited by administration of D-GalN through

Table 3
^{1}H and ^{13}C NMR spectroscopic data (pyridine-d_5) of **3**.

	3	
Position	δ_H	δ_C
1	1.27 (br d, *ca.* 13)	48.1
	2.26 (dd, 4.5, 12.5)	
2	4.09 (dd, 4.5, 9.4)	68.7
3	3.37 (d, 9.4)	84.0
4		39.9
5	1.07 (m)	56.1
6	1.45 (m)	19.1
	1.56 (m)	
7	1.47 (m)	33.6
	1.66 (m)	
8		40.7
9	1.94 (m)	47.9
10		38.6
11	2.13 (2H, m)	24.2
12	5.55 (dd, 3.5, 3.5)	128.5
13		139.3
14		42.2
15	1.25 (m)	29.2
	2.43 (ddd, 4.7, 13.0, 14.1)	
16	2.00 (m)	26.2
	3.06 (ddd, 4.4, 13.0, 13.2)	
17		48.8
18	2.92 (br s)	54.4
19		72.7
20	1.33 (m)	42.1
21	1.22 (m)	26.7
	1.96 (m)	
22	1.96 (m)	37.8
	2.07 (m)	
23	1.25 (3H, s)	29.4
24	1.09 (3H, s)	17.6
25	1.10 (3H, s)	17.1
26	1.19 (3H, s)	17.6
27	1.66 (3H, s)	24.6
28		176.9
29	1.37 (3H, s)	27.0
30	1.04 (3H, d, 6.5)	16.6
28-*O*-Glc		
1′	6.22 (d, 7.9)	95.7
2′	4.21 (dd, 7.9, 8.9)	74.0
3′	4.25 (dd, 8.0, 8.9)	78.7
4′	4.11 (m)	71.2
5′	4.11 (m)	76.1
6′	4.76 (m)	64.5
	4.86 (dd, 1.7, 12.2)	
6′-*O*-Ac		170.8
	1.95 (3H, s)	20.7

depletion of uridine triphosphate in hepatocytes. Second, pro-inflammatory mediators, such as nitric oxide (NO) and tumor necrosis factor-α (TNF-α), are released from LPS-activated macrophages (Kupffer's cells). Apoptosis of hepatocytes by TNF-α is reported to play an important role in this D-GalN/LPS-induced liver injury (Josephs et al., 2000). In a previous investigation of compounds from natural medicines possessing hepatoprotective activity, it was reported that sesquiterpenes and diarylheptanoids from *Curcuma zedoaria* (Morikawa et al., 2002), acid amides from *Piper chaba* (Matsuda et al., 2009) and acylated phenylethanoids from *C. tubulosa* (Morikawa et al., 2010a) exhibited significant protective effects against liver injuries induced by D-GalN/LPS in mice. In addition, these constituents were found to reduce D-GalN-induced cytotoxicity in primary cultured hepatocytes. Because a methanol extract of the tuberous roots of *P. anserina* also exhibited hepatoprotective effects in this study, the inhibitory effects of its constituents on D-GalN/LPS-induced cytotoxicity were examined in primary cultured mouse hepatocytes by the 3-(4,5-dimethylthiazol-2-yl)-2,5-diphenyltetrazolium bromide (MTT) assay. Thus, we found that the following four triterpenes: potentillanoside A (**1**, IC_{50} = 46.7 μM), tormentic acid (**9**, 9.5 μM), rosamutin (**10**, 35.5 μM), and kaji-ichigoside F1 (**12**, 14.1 μM) and gallic acid methylester (53.7 μM), (+)-catechin (17.7 μM), (+)-gallocatechin (18.4 μM), (+)-catechin 7-*O*-β-D-glucopyranoside (55.4 μM), and quercetin 3-*O*-β-D-glucopyranoside (34.2 μM) exhibited significant activity. Among the triterpene constituents, the potency of **9**, **10**, and **12** was higher than that of silybin (38.8 μM), a commercially available positive control (Fehér et al., 1989; Skottová and Krecman, 1998) (Table 6).

Effects on LPS-activated NO production in mouse peritoneal macrophages

Effects of the isolates on NO production were examined to provide an index for estimation of macrophage activating levels in LPS-treated mouse peritoneal macrophages. Thus, it was found that pomolic acid (**7**, IC_{50} = 33.1 μM), 28-*O*-β-D-glucopyranosyl pomolic acid (**8**, 91.9 μM), **9** (68.4 μM), 2α-hydroxyursolic acid (**16**, 21.1 μM), and maslinic acid (**18**, 30.1 μM) significantly inhibited NO production (Table 7). The potencies of **7**, **16**, and **18** were equivalent to that of N^G-monomethyl-L-arginine (L-NMMA, 36.0 μM), a NO synthase inhibitor, but were lower than that of caffeic acid phenethyl ester (CAPE, 11.0 μM), an inhibitor of nuclear factor-κB activation (Morikawa et al., 2011). Thus, these compounds were found to prevent overproductions of NO from LPS-activated macrophages.

Effects on TNF-α-induced cytotoxicity in L929 cells

To examine the effects of the constituents on TNF-α-induced cytotoxicity, the viability of L929 cells, a TNF-α-sensitive cell line (Kouroku et al., 2000), under the presence of the constituents was examined. Thus, it was found that only **8** (IC_{50} = 25.5 μM) significantly improved cell viability (Table 8).

*Effects of principal triterpenes (**1**, **7**, **9**, **10**, and **12**) on D-GalN/LPS-induced liver injuries in mice*

Finally, the effects of the principal triterpenes: potentillanoside A (**1**), pomolic acid (**7**), tormentic acid (**9**), rosamutin (**10**), and kaji-ichigoside F1 (**12**) on D-GalN/LPS-induced liver injuries in mice were examined. Three ursane-type triterpene 28-*O*-monoglycosyl esters (**1**, **10**, and **12**) were found to significantly inhibit the increase in both sAST and sALT levels induced by D-GalN/LPS in mice at doses of 50–100 mg/kg, p.o. In particular, the inhibitory activity of **1** was significant and was as potent as curcumin, a positive control (Morikawa et al., 2002) (Table 9).

Concluding remarks

In conclusion, a methanol extracts from the tuberous roots of *P. anserina* exhibited protective effects against liver injuries induced by D-GalN/LPS in mice. From the extract, six new triterpene 28-*O*-monoglucopyranosyl esters, potentillanosides A–F (**1**–**6**) were isolated along with 32 known compounds, including 15 triterpenes (**7**–**21**). Among the isolated constituents, three ursane-type triterpene 28-*O*-monoglycosyl esters (**1**, **10**, and **12**) showed *in vivo* hepatoprotective effects at doses of 50–100 mg/kg, p.o. On the basis of *in vitro* studies, the following plausible mechanisms of action for the hepatoprotective effect can be proposed: (i) reduction of both D-GalN and TNF-α-induced cytotoxicity (**8**), (ii) reduction of D-GalN induced cytotoxicity (**1**, **10**, and **12**), and (iii) inhibition of LPS-activated macrophage activation (**7**, **9**, **16**, and **18**). However, the detailed mechanisms of action for the hepatoprotective effect need to be studied further.